The meningococcal vaccine antigen GNA2091 is an analogue of YraP and plays key roles in outer membrane stability and virulence.

Kate L. Seib*, Andreas F. Haag[‡1], Francesca Oriente[‡], Laura Fantappiè[‡2], Sara Borghi[3], Evgeny A. Semchenko*, Benjamin L. Schulz[#], Francesca Ferlicca[‡], Anna Rita Taddei[†], Marzia Giuliani[‡], Mariagrazia Pizza[‡], Isabel Delany[‡4]

*Institute for Glycomics, Griffith University, Gold Coast, Australia

[‡]GSK Vaccines, Siena, Italy

[#]School of Chemistry and Molecular Biosciences, The University of Queensland, Brisbane, Australia

[†]Interdepartmental Centre of Electron Microscopy CIME, Tuscia University, Tuscia, Italy

[1] Current affiliation: Institute of Infection, Immunity and Inflammation, College of Medical, Veterinary and Life Sciences, University of Glasgow, Glasgow, UK.

[2] Current affiliation: Toscana Life Sciences, Via Fiorentina 1, 53100 Siena, Italy.

[3] Current affiliation: Laboratory of Molecular Genetics and Immunology, The Rockefeller University, New York, NY 10065, USA.

[4] Correspondence: GSK Vaccines, Via Fiorentina 1, 53100 Siena, Italy.
E-mail: Isabel.x.delany@gsk.com

Short title: Role of GNA2091 in meningococcal membrane stability

Nonstandard abbreviations

4CMenB: Four component meningococcal serogroup B vaccine.

CFU: colony forming units

CI: competitive index

LOS: lipooligosaccharide

LPS: lipopolysaccharide

OMP: outer membrane protein

OMV: outer membrane vesicle

qRT-PCR: quantitative real time polymerase chain reaction

SBA: serum bactericidal activity

Abstract

GNA2091 is one of the components of the 4CMenB vaccine and is highly conserved in all meningococcal strains. However, its functional role has not been fully characterized. Here we show that *nmb2091* is part of an operon, and is co-transcribed with the *nmb2089, nmb2090* and *nmb2092* adjacent genes, and a similar but reduced operon arrangement is conserved in many other Gram negative bacteria. Deletion of the *nmb2091* gene causes an aggregative phenotype with a mild defect in cell separation; differences in the outer membrane composition and phospholipid profile, in particular in the phosphoethanolamine levels; an increased level of outer membrane vesicles; and deregulation of the zinc-responsive genes such as *znuD*. Finally, the Δ2091 strain is attenuated with respect to the wild type strain in competitive index experiments in the infant rat model of meningococcal infection. Altogether these data suggest that GNA2091 plays important roles in outer membrane architecture, biogenesis, homeostasis, and in meningococcal survival *in vivo* and a model for its role is discussed. These findings highlight the importance of GNA2091 as vaccine component.

Keywords: Bexsero, 4CMenB, outer membrane, phospholipid, zinc

Introduction

Neisseria meningitidis, a Gram-negative β-proteobacteria, is a leading cause of bacterial sepsis and meningitis worldwide (1). The meningococcal protein GNA2091 was first described during the *N. meningitidis* serogroup B (MenB) reverse vaccinology project as a lipoprotein predicted to be surface exposed in some meningococcal strains, which is able to induce passive protection in the

adult mouse model of meningococcal bacteraemia (2). The function of GNA2091 is still unknown but due to its protective properties it was selected for inclusion in the 4CMenB vaccine (trade name Bexsero) (3).

The 4CMenB vaccine is widely licensed and used to protect against invasive meningococcal disease from MenB and has also been introduced in the UK for mass vaccination of infants (4). 4CMenB contains three recombinant proteins (fHbp, NHBA and NadA) and outer membrane vesicles (OMVs) derived from New Zealand strain NZ 98/254 (2, 5). The immunogenicity and stability of the recombinant antigens was optimized by generating protein-protein fusions of fHbp-GNA2091 and NHBA-GNA1030, which induce higher serum bactericidal activity (SBA) titers than those induced by the individual antigens alone (2). fHbp, NadA and NHBA have been extensively characterised and shown to be involved in meningococcal virulence (6-11). The accessory protein GNA1030 has recently been characterised as a Neisseria ubiquinone binding protein (NUbp) (12). However, the role of GNA2091 has not yet been characterized in detail.

GNA2091 has been shown to be localized at the periplasmic side of the outer membrane, where it is proposed to be required for the efficient assembly of a subset of outer membrane proteins (OMPs), including PorA, PorB, PilQ and the Bam complex, with accumulation of misassembled monomeric proteins seen in a *gna2091* mutant strain (13). The *gna2091* mutant is also sensitive to detergent stress, indicating compromised membrane integrity (14). Here we further characterise the expression and functional role of GNA2091 *in vitro* and in the *in vivo* infant rat model of meningococcal bacteraemia.

Materials and Methods

Strains and culture conditions

The MC58 wild type, the MC58Δ2091 mutant strain and the MC58Δ2091_C complemented strain, have been previously described (14). Strains 2996Δ2091 and 2996Δ2091_C were generated by transformation of 2996 with the plasmids pBSUD936::Erm and pComP$_{RBS}$936::Cm, as previously described (14).

N. meningitidis strains were routinely grown on GC agar or Mueller-Hinton (MH) agar at 37°C and 5% CO_2 overnight. Columbia agar was used for growth of bacteria recovered from infant rat experiments. For liquid cultures, overnight growth was used to inoculate GC or MH broth. *Escherichia coli* strains used for cloning were cultured in Luria-Bertani (LB) broth or on LB agar. When required, erythromycin and/or chloramphenicol was added to achieve a final concentration of 5 μg ml^{-1}. Growth rate experiments were performed as previously described by following the optical density at 600 nm (OD_{600}) (14). Bacterial aggregation experiments were performed by selecting at least six single colonies and suspending them independently in GC broth, or taking samples of equal OD from liquid growth, then the number of viable colony-forming units (CFU) was determined by plating serial dilutions onto MH agar. All experiments were performed in triplicate and on at least three occasions. Statistical analysis was performed using the Student's t-test.

General molecular biology and bioinformatic techniques

Techniques including PCR, cloning, SDS-PAGE, Western Blot and flow cytometry analysis were performed as previously described (14, 15). The NCBI Basic Local Alignment Search Tool (BLASTn or BLASTp) was used to identify nucleotide and protein sequence homologues, respectively. Sequence alignments were performed using ClustalW and were exported into Jalview to generate the alignment figure.

Reverse transcription PCR (RT-PCR)

RNA extraction was performed as previously described and 2µg of total RNA was reverse transcribed with random primers and SuperScript II reverse transcriptase (Invitrogen). The resulting cDNA was amplified using primer pairs (Table S1) specific for *gna2091* (2091rtF2 and 2091rtR2) and for the intergenic regions of the genes from *gna2089* to gna2093 (2089rtF and 2090rtR; 2090rtF and 2091rtR2; 2091rtF2 and 2092rtR; 2092rtF and 2093rtR). For each primer pair, an RNA-containing reaction in which the reverse transcriptase step was omitted was used as a negative control for DNA contamination, and genomic DNA was used as a positive control.

Microarray analysis and quantitative real time PCR (qRT-PCR)

Triplicate cultures of MC58 wild type and Δ2091 mutant strains were grown to early-exponential phase (OD_{600} 0.2) in MH broth. RNA extraction, cDNA preparation and microarray analysis was performed as previously described (16). Experiments were performed with cDNA from three pools (*i.e.,* RNA extracted from nine-independent cultures for each strain), with a dye-swap. Relative gene expression between the wild type and mutant strains was confirmed for a selection of genes using quantitative real time PCR (qRT-PCR) with cDNA from triplicate RNA samples and primers shown in Table S1, as previously described (16).

Scanning electron microscopy and thin section transmission electron microscopy (TEM)

N. meningitidis strains were harvested into phosphate buffered saline (PBS) and washed three times (5 min, 2000 × *g* centrifugation). Samples containing ~$1x10^6$ CFU were fixed on plastic cover slips with 2% glutaraldehyde / 5% formaldehyde solution for 10 min at room temperature. Cover slips were washed three times with H_2O, dehydrated in ethanol (15, 30, 50, 75, 90 and 100%) and hexamethyldisilazane (50% ethanol/HMDS then 100% HMDS). Samples were coated with ~6nm gold prior to analysis on Jeol 5000 Scanning Electron Microscope.

For thin section TEM, Samples were fixed with a mixture of 0.5% glutaraldehyde and 4% paraformaldehyde in 0.1 M phosphate buffer, pH 6.9 for 20 min at room temperature. After rinsing in the same buffer for 10 min, samples were dehydrated in a graded ethanol series and embedded in medium grade LR white resin. The resin was polymerised in tightly capped gelatine capsules for 24 h at 50°C. Ultrathin sections were obtained using a Reichert Ultracut ultramicrotome with a diamond knife, and collected on nickel grids. Sections were subsequently stained with uranyl acetate and lead citrate and observed with a Jeol JEM EX II transmission electron microscope at 100 kV.

Outer membrane vesicle (OMV) preparation and outer membrane protein (OMP) quantification

OMVs were isolated from bacterial culture supernatants as described previously, with the following modifications (17). Briefly, bacteria were inoculated in 500 ml baffled flasks containing 150 ml Meningitidis Chemically Defined Medium I (MCDMI), grown with shaking at 180 rpm at 37 °C for 16 h and then centrifuged at 3200 × *g* for 30 min at 4 °C. The supernatants were filtered through 0.2 µm pore size Stericup filters (Millipore Express Plus) followed by ultra-centrifugation at 100,000 × *g* for 2 h at 4 °C (rotor 45 Ti, Beckman). Pellets were washed with PBS and ultracentrifugation was repeated. The final pellets were re-suspended in 500 µl PBS and protein quantified using the DC Protein Assay (Bio-Rad) according to manufacturer's instructions.

Lipid extraction and thin layer chromatography (TLC) analysis

OMVs (20 µg based on protein content) were used to extract lipids as described previously (18), with the following modifications. Briefly, one volume of methanol was added to the OMVs and samples were gently mixed using a thermal shaker for 15 min at 25°C to complete protein denaturation. One volume of chloroform was then added, and samples were incubated for 15 min at 25°C under gentle agitation. The samples were then centrifuged at 2000 x *g* for 10 min to obtain complete partitioning of lipids into the organic phase, which was collected into a new tube and

dried by applying nitrogen flow. Lipids were resuspended in 100 µl of chloroform and stored at -80°C until use. For TLC separation, lipids were loaded on aluminium backed 50*75 mm TLC Silica gel 60 F254 plates (layer thickness 200 µm) and resolved in vertical developing TLC chamber using a running buffer composed by chloroform, ethanol, water and trimethylamine (35:35:7:35, v/v). Lipids were visualized using a solution of primulin (0.05% w/v in a solution of acetone and water 8:2) (19) and visualised under UV light.

Phospholipid preparation and mass spectrophotometry (MS) analysis

Bacteria from overnight growth were used to extract phospholipids as described previously (20). Briefly, bacteria were collected and washed once in HPLC grade water, freeze dried, resuspended in 1 mL of chloroform/methanol solvent (2:1 v/v), incubated for 30 min at 25°C, then centrifuged and the supernatant collected. Extraction was repeated one more time. The supernatant was then mixed with 2 volumes of Folch upper phase reagent (chloroform/methanol/water containing 0.74% potassium chloride, 3:48:47 by volume) and vortexed. The lower phase was collected and the extraction repeated three times, before being dried by applying nitrogen flow, weighed and stored at -80˚C.

Lipids were diluted to 1 µg/µl in chloroform/methanol (2:1). Samples were infused on a TripleTof 5600 mass spectrometer (SCIEX) at a flow rate of 200 nl/min using a Nanospray III source. Ionisation conditions included: Gas 1 = 6 psi, Cur = 30 psi, heater = 150 °C, ISFV = 4000 V. Data was acquired using the MSMS^{all} script. MS was performed across 200 – 2000 *m/z* for 10 s, followed by MS/MS across 200 – 1250 *m/z* in 1 Da steps, acquired for 500 ms per step. For MS/MS, CE was set to 50 with spread +/- 30V. Analysis was performed separately in both positive and negative modes.

In vivo infant rat model of meningococcal infection

The infant rat model competitive index (CI) was used as previously described (14). Briefly, bacteria were grown to early-exponential phase (OD_{600} 0.2) in GC medium, washed, and resuspended in PBS. Five to six-day-old pups from litters of outbred Wistar rats (Charles River) were challenged intraperitoneally with a 1:1 mix of the 2996 wild type and 2996Δ2091 mutant strains, or the 2996Δ2091_C complemented and 2996Δ2091 mutant strains, at an infectious dose of $1x10^3$, $1x10^4$ or $1x10^5$ CFU. A control group of infant rats was injected with PBS. Eighteen hours after the bacterial challenge, blood samples were obtained by cheek puncture, and aliquots were plated onto columbia agar + 5% horse blood and columbia agar + 5% horse blood plus erythromycin or chloramphenicol (to select for 2996Δ2091 or 2996Δ2091_C bacteria, respectively) for viable cell counting. The numbers of CFU/ml of blood were determined after overnight incubation and the CI ratio calculated using the following formula: CI = (wild type CFU recovered / mutant CFU recovered) / (wild type inoculum /mutant inoculum). Statistical analysis was performed using the two-tailed Wilcoxon Signed-Ranks Test.

Results

Characterisation of the *GNA2091* gene locus in *N. meningitidis*

GNA2091 is a lipoprotein of 202 amino acids (predicted MW ~22kDa) (Fig. 1A), BLASTp search revealed matches (≥64% identity) to GNA2091 homologues not only in *Neisseria meningitidis* and *Neisseria gonorrhoeae*, but also in other *Neisseria* species, as well as matches (≤55% identity) in several other bacterial species. There is 24-28% identity (43-49% similarity) between GNA2091 and its orthologues, including YraP of *E. coli* (Fig. 1D). GNA2091 has been described as containing a single BON (bacterial OsmY and nodulation) domain (Pfam; PF04972) (13). However, our analysis of PROSITE indicates the presence of two BON domains, from amino acid 53-123 and 133-202 (Fig. 1A). BON domains have an unknown role but are postulated to be involved in

phospholipid-binding (21). GNA2091 also has a significant match from amino acid 1-200 with the OsmY (predicted periplasmic or secreted lipoprotein) NCBI Conserved Doman family [COG2823].

GNA2091 is encoded by the 609 bp gene *nmb2091* in *N. meningitidis* strain MC58 (22) (Fig. 1B). Reverse transcriptase PCR (RT-PCR) analysis on total RNA from strain MC58 revealed an amplification product across the intergenic regions between the genes *nmb2089, nmb2090, nmb2091* and *nmb2092* (Fig. 1C), suggesting that the *nmb2091* gene is included in an operon and is co-transcribed with two upstream and one downstream gene. The genes adjacent to *nmb2091* are annotated as follows: *nmb2089*- a conserved hypothetical protein that has putative conserved domains matching COG0792 (predicted endonuclease domain); *nmb2090*- a homologue of phosphoheptose isomerase *gmhA* that is involved in the first step of the biosynthesis of Gram-negative bacteria inner core lipooligosaccharide (LOS) precursor, L-glycero-D-mannoheptose (23); and *nmb2092*- a hypothetical protein. Interestingly, further analysis of this genomic region revealed that several Gram-negative bacteria have a similar three gene arrangement, matching *nmb2089, nmb2090, nmb2091 genes*, while *nmb2092*, with an unknown function, appears to be *Neisseria* specific.

The GNA2091 mutant strain displays increased aggregation, likely due to a mild cell separation deficiency

To evaluate the influence of GNA2091 on bacterial growth *in vitro*, the wild-type, the Δ2091 mutant strain and a complemented strain were grown in GC broth and agar, and analysed for growth rate, bacterial count and by electron microscopy. During the time course of these experiments, we observed that the growth of the three strains was identical in terms of OD (Fig. 2A), but that the mutant strain yielded fewer CFU ml^{-1} than the wild type or the Δ2091_C strains, when comparing CFU from single colonies (Fig. 2B) or from growth in liquid media at equivalent ODs (data not shown). Cell aggregation was not visible to the eye during liquid culture, however scanning

electron microscopy (SEM) revealed that while the wild type and complemented strains were typically visualised as cocci or diplococci, the Δ2091 mutant formed larger aggregates of bacteria (Fig. 2C), suggesting that the deletion of the *gna2091* gene may cause an alteration of the bacterial surface or cell separation. Thin-section transmission electron microscopy (TEM) revealed that the knockout has a mild defect in cell separation and while both wild type and complemented strains clearly are present as single cocci or diplococci, there is a tendency for the mutant to form tetrads or triads, and on occasions larger clusters with formed septa but which may fail to separate (Fig. 2D).

GNA2091 is involved in outer membrane homeostasis, with altered OMP, OMV and phospholipid levels seen in the GNA2091 mutant strain

We analysed the composition of membrane LOS, phospholipids, integral membrane proteins and lipoproteins in *N. meningitidis* MC58, Δ2091 and Δ2091_C strains grown to mid-log in GC broth. Whole-cell lysates and OMVs of wild type, mutant and complemented strains were prepared and analysed by SDS-PAGE and Western blot with polyclonal mouse sera raised to OMVs. No differences were seen in the overall banding pattern from whole cell lysates of the three strains, on either the Coomassie stained SDS-PAGE or Western blot (Fig. 3A). However, several differences were evident in the OMV preparations of the Δ2091 mutant strain compared to the wild type and complemented strains (Fig. 3B). The three major bands detected on the Coomassie stained SDS-PAGE (corresponding to PorB, and Opa/Opc proteins) were present at a higher level in the Δ2091 mutant strain, and Western blot analysis of a duplicate gel probed with anti-OMV antisera indicated a significantly different antibody recognition pattern in the Δ2091 mutant, with increased expression of several bands compared to the wild type and Δ2091_C strains (Fig. 3B). The yield of OMVs released, measured as total protein ml^{-1} of culture supernatant processed, was also found to be approximately 10-fold higher in the Δ2091 mutant relative to wild type and complemented cultures (Fig. 3C). Hypervesiculation of the Δ2091 mutant strain was confirmed by scanning electron micrography (Fig. 3D)

GNA2091 contains two BON domains (Fig. 1A). While the function of BON domains is unknown, they are proposed to play a role in phospholipid binding (21). To investigate whether the phospholipid content of the outer membrane of *N. meningitidis* was altered in the absence of GNA2091, phospholipids were isolated from wild type, Δ2091 and Δ2091_C whole cells and OMV preparations and analysed by thin-layer chromatography and mass spectrometry. Using identical quantities of OMV phospholipid extract, we observed that the phospholipid composition of the Δ2091 mutant was altered, with an upper band missing and an increase in a lower band relative to the wild type and complemented strains (Fig. 4A). MS/MS on whole cell samples confirmed an altered phospholipid composition between the strains, with an increased abundance of 1-(9Z-hexadecenoyl)-2-hexadecanoyl-glycero-3-phosphoethanolamine PE(16:1(9Z)/16:0) in the Δ2091 mutant strain relative to the wild type and complemented strains (Fig. 4B-D). Together, these data indicate that GNA2091 affects OMP, OMV and phospholipid composition in *N. meningitidis*.

GNA2091 is co-transcribed with *nmb2090* (encodes GmhA), an enzyme involved in the biosynthesis of the LOS inner core, suggesting the GNA2091 may be involved in LOS synthesis. However, SDS-PAGE and silver staining of LOS extracted from the wild type, mutant and complemented strains (during early exponential growth, with all strains in the same growth phase) showed consistent LOS profiles between these strains (data not shown). No difference in capsule was detected between the three strains, as determined by flow cytometry with anticapsular monoclonal antibody SEAM12 (data not shown).

Microarray analysis reveals induction of the zinc regulon in the GNA2091 mutant strain

Although the *N. meningitidis* MC58Δ2091 mutant strain has normal growth in GC (0.4% glucose w/v), it has previously been shown that the mutant strains decreased growth in MH (no glucose added) relative to the wild type strain, and that this growth defect can be relieved by addition of

glucose (14). To gain further insight into the role of GNA2091 and the basis of these growth phenotypes, the MC58 wild type and Δ2091 strains were compared by microarray analysis using a meningococcal genome array. The strains were grown in MH broth to an OD_{600} of 0.2, which is just before the growth defect of Δ2091 is evident (Fig. 5A), and RNA extracted. A total of 20 genes had ≥2 fold altered expression between the wild type and Δ2091 mutant strains; 15 genes had increased expression in Δ2091, while five genes had decreased expression in Δ2091 (Table S2). Microarray results were validated by qRT-PCR of a selection of regulated genes, or by Western blot analysis or flow cytometry (Table S2). The majority of regulated genes are involved in zinc or iron homeostasis, or metabolism (Fig. 5B). Figure 5B shows the overlap of regulated genes with nine members of the *N. meningitidis* Zur (Zn uptake regulator) regulon (24) or the *N. gonorrhoeae* Zur regulon (originally described as the Mn uptake regulator PerR) (25), and five members of the Fur (ferric uptake regulator) regulated genes (26, 27). Almost the complete Zur regulon has altered expression in the Δ2091 strain, suggesting that there is a decreased intracellular zinc concentration in the absence of GNA2091.

Decreased growth in the GNA2091 mutant strain can be rescued by zinc

Based on the microarray results obtained, we further investigated the growth of the wild type, Δ2091 mutant and Δ2091_C complemented strains in MH media supplemented with zinc. Figure 5A shows that addition of zinc to MH broth is able rescue the growth defect of the Δ2091 mutant strain. The ability of zinc to restore growth was also confirmed in the Δ2091 mutant of *N. meningitidis* strain 2996 (data not shown).

Expression of *znuD*, which encodes the zinc uptake protein ZnuD that is upregulated under low Zn conditions (28), was investigated as a marker of intracellular zinc concentrations in the wild type, Δ2091 mutant and Δ2091_C complemented strains. qRT-PCR analysis revealed a 12-fold increase in expression of *znuD* in the Δ2091 strain grown in MH compared to the wild type strain, with

normal *znuD* expression restored in the complemented strain (Fig. 5C). When zinc is added to the media, *znuD* expression is repressed in all 3 strains, with restoration of the normal wild type *znuD* expression profile in the mutant strain. These findings suggest that GNA2091 plays a role in the efficient uptake of zinc into the cell during growth in low zinc conditions.

GNA2091 is required for survival in the infant rat model of meningococcal infection

Changes in the bacterial cell membrane and efficiency of nutrient uptake often affect how bacteria can interact with their host. In order to examine the role of GNA2091 *in vivo*, the fitness of the *N. meningitidis* 2996 (a strain adapted for infant rat infection) was investigated in the infant rat model of meningococcal infection using a competitive index (CI) assay. *N. meningitidis* 2996 wild type and Δ2091 mutant bacteria were injected intraperitoneally at a ratio of 1:1, at infectious doses of $1x10^3$, $1x10^4$ or $1x10^5$ CFU, to determine if the wild type bacteria could out-compete the Δ2091 bacteria. Bacterial CFU in the blood were determined after 18 hrs and a CI of <1 was seen for almost all rats in each group indicating that the mutant Δ2091 bacteria had decreased survival with respect to the wild type (Fig. 6; mean CI of 0.42, 0.36 and 0.32 with an infectious dose of $1x10^3$, $1x10^4$ and $1x10^5$ CFU, respectively). Furthermore, the wild type phenotype was partially restored in the complemented strain. This suggests that a functional GNA2091 is required for optimal growth and survival of *N. meningitidis in vivo*.

Discussion

The *N. meningitidis* protein GNA2091 is a component of the serogroup B meningococcal vaccine 4CMenB (Bexsero), and is present as a fusion protein with fHbp (2, 5). The fHbp-GNA2091 fusion protein has increased immunogenicity and stability relative to fHbp alone (2). Previously it has been shown that GNA2091 is required for optimal growth in minimal media and for resistance to

membrane stress (14). GNA2091 has also been proposed to be required for the efficient assembly of a subset of OMPs, including PorA, PorB, PilQ and others (13). Here we expand the characterization of the function of GNA2019 and suggest that it plays a broader role in outer membrane biogenesis and/or homeostasis than previously described.

The Gram-negative bacterial outer membrane is a complex biological barrier that is composed of an asymmetric lipid bilayer, with LOS or lipopolysaccharide (LPS) in the outer leaflet and phospholipids in the inner leaflet, as well as integral membrane proteins and lipoproteins. Outer membrane biogenesis is complex and involves several pathways including the Lpt complex for LOS or LPS, the Lol and Slam pathways for lipoproteins, the Bam and Tam complexes for OMPs, and a network of chaperones (reviewed in 29, 30, 31). Phospholipid transport to the outer membrane remains relatively poorly understood, but involves the Mla pathway genes, so called initially for their role in maintenance of OM lipid asymmetry (32) and recently described as a lipid transport system and also known as the MCE protein superfamily (33). Here we show that the deletion of GNA2091 results in several phenotypes in *N. meningitidis* that indicate it is involved in OM biogenesis and/or homeostasis, and that result in reduced fitness in an infant rat infection model. While GNA2091 is not an essential protein for the growth or survival of *N. meningitidis* (13, 14), the importance of its functional role is supported by the fact that the gene encoding GNA2091 is well conserved and always in frame in the genus *Neisseria* (34). Specifically, it is highly conserved in *N. meningitidis* (34, 35) and *N. gonorrhoeae* (34, 36) and the gene is present in all commensal *Neisseria* species investigated, including *Neisseria lactamica, Neisseria polysaccharea, Neisseria flavescens, Neisseria cinerea* (34) and *Neisseria weaveri* (34; unpublished GenBank search). GNA2091 is constitutively expressed during growth in broth (14), but is upregulated during growth at 32°C versus 37°C (37) and during growth in blood (38), consistent with conditions seen during nasopharyngeal colonization and invasive disease, respectively. Here we show that GNA2091 is expressed as part of a four gene operon (nmb2089-nmb2092) conserved in *Neisseria* spp. The first three genes are conserved across many Gram negative bacteria and may play a role in envelope

biogenesis across the genera. The gene nmb2090 encodes a homologue of phosphoheptose isomerase GmhA that is involved in the biosynthesis of LOS (23). The genes nmb2089 and nmb2092 are hypothetical proteins, the latter specific to *Neisseria*, and elucidation of their functions may reveal additional details of the role of GNA2091.

GNA2091 contains two bacterial OsmY and nodulation (BON) domains, which have an unknown role but are considered to have a structural rather than a catalytic function, in particular they are believed to be involved in phospholipid binding (21). The BON domain is typically ~60 residues long with an alpha/beta predicted fold, a conserved glycine residue and several hydrophobic regions. BON domains are found in a family of osmotic shock protection proteins (21) that includes the OsmY protein of *E. coli,* which is expressed in response to various stress conditions and is involved in protection against osmotic shock (39). The GNA2091 homolog in *E. coli*, YraP, also contains BON domains and a *yraP* knockout strain has a detergent-sensitive phenotype (40), similar to the *N. meningitidis gna2091* knockout (14). In *E. coli,* YraP is believed to be involved in a periplasmic protein folding pathway that functions in parallel to the chaperone protein SurA, since there is synthetic lethality between *yraP* and *surA* mutations (40). However, in *N. meningitidis*, the *sur*A single mutant is not noticeably affected in OMP assembly (41), and no synthetic defects were seen in the *surA* / GNA2091 double mutant (13). Although there were higher levels of unassembled porins in a double mutant of GNA2091 and the chaperone Skp (13). YraP of *E. coli* is also involved in cell division, and is believed to be recruited to the divisome following cell constriction where it is involved in NlpD and AmiC activation by an as yet unknown mechanism (42). The divisome is a ring-shaped cytokinetic apparatus that contains dozens of proteins involved in cell division, and while a single Δ*yraP* mutant divided normally and a single Δ*envC* mutant had a mild separation phenotype, a Δ*envC* Δ*yraP* mutant resulted in a severe chaining defect (42). Here we show that the GNA2091 mutant has a mild cell separation phenotype resembling that of *Neisseria* spp. with defects in AmiC amidase protein (43). Interestingly, while *E. coli* have three amidase proteins,

AmiC is the unique cell separation amidase in *Neisseria.* Therefore both YraP from *E. coli* and GNA2091 have an affect on cell separation that may be through lack of AmiC activation.

The GNA2019 mutant exhibits an increased blebbing or yield of OMVs as well as an altered level and/or altered immune recognition of several OMV proteins. This is consistent with the increased protein level seen by Bos *et al.* in the culture supernatant of the GNA2091 mutant (13). The increased blebbing may be a consequence of the cell separation phenotype as defects in cell separation for other bacteria result in hypervesiculation (44, 45). On the other hand, an increase in the relative proportion of PE may also induce stress and disrupt the OM bilayer, as PE is able to form non-bilayer structures due to its curvature (46) and essentially result in hypervesiculation (47).

The role of YraP has also recently been investigated in *Salmonella enterica* Serovar Typhimurium, where a *yraP* mutant had increased sensitivity to anionic compounds and attenuated virulence in an oral infection model and during the early stages of systemic infection (48). The YraP mutation is proposed to result in a defective outer membrane barrier, and since levels of lipopolysaccharide, O antigen and major OMPs were not affected in *S. enterica* it was suggested that other membrane components, such as phospholipids, may be affected (48). As of May 2019 the BON family contains 13009 sequences from 3394 species and there are 64 different Bon domain architectures, and 1983 sequences in the Pfam database with a BONx2 architecture similar to that seen in GNA2091. It has been reported that most proteobacteria have one or two BON containing proteins (49) and our recent searches indicate that GNA2091 is the only BON containing protein in *N. meningitidis* presently in the Pfam database. Due to the sequence and functional similarities between GNA2091 and YraP of *E. coli*, we propose that GNA2091 be named YraP from herein also in *Neisseria* spp.

The phenotypes seen for the meningococcal YraP mutant described herein and previously (13, 14), may be due to changes in the phospholipid composition of the membrane resulting from the absence of YraP and BON domain-mediated phospholipid binding. Although the specific mechanism of YraP in outer membrane biogenesis remains unknown, the phenotype of the mutant holds much in

common with the phenotype described for many Gram negative bacteria lacking a functional phospholipid transport system (32, 47). Mutants of a functional Mla system were shown to result in hypervesiculation of OM vesicles with increased PE (47) similar to what we describe here for the YraP mutant. We show also that there is an interplay between YraP, phospholipids, OMVs, OMPs, and zinc. The phospholipid composition of the YraP mutant is altered, with an increased level of phosphoethanolamine (PE(16:1(9Z)/16:0)). In *N. meningitidis*, phosphatidylethanolamine (PE) is the major phospholipid, followed by phosphatidylglycerol (PG), and there are minor amounts of phosphatidic acid (PA) and trace levels of cardiolipin (DPG) (20). The altered phospholipid content of the OM of the mutant may explain the report by Bos *et al.* that there are a subset of proteins in the YraP mutant which are misassembled in the OM (13). Several properties of phospholipids affect membrane protein assembly and function, including their hydrophobicity, charge, rigidity and radius of curvature (50). The ratio of PE, PG and phosphatidylcholine (PC) in vesicles can affect the rate of protein folding and membrane insertion (50, 51) and protein topology (52). For example, the absence of PE in *E. coli* affects cell division resulting in filamentous cells (46), and also causes the misfolding of sugar and amino acid transporters (46), including lactose permease (LacY) (53, 54). The YraP mutant shows upregulation of several genes, including the majority of genes in the zinc regulon, suggesting low internal Zn concentrations leading also to decreased growth of the mutant in low zinc conditions. Furthermore, the induction of the zinc regulon can be reversed by the addition of zinc to the media, suggesting that zinc uptake remains intact in the mutant, but that it is inefficient. This is consistent with a decreased efficiency of zinc-transporter functions in the mutant strain. While there are many direct links between zinc and phospholipids (55-57), the model we propose for the role of YraP is that in *N. meningitidis* wild type cells that express YraP, phospholipids are correctly incorporated into the outer membrane and enable normal recruitment, formation, stabilization and/or functional activity of outer membrane proteins, including ZnuD. However, in the absence of YraP in the Δ2091 mutant strains, the outer membrane phospholipid composition of *N. meningitidis* is altered and outer membrane protein assembly and/or function is

456 altered for a number of proteins including ZnuD which in turn effects efficient Zinc uptake.
457 Interestingly, the cell separation AmiC protein uses a zinc cofactor (43). The zinc transport
458 deficiency that we observed in the YraP mutant may therefore result in reduced function of AmiC
459 and thereby give one plausible explanation for the cell separation phenotype of the mutant.
460 In summary, the outer membrane lipoprotein GNA2091, herein called YraP, is involved in outer
461 membrane biogenesis and/or homeostasis, as indicated by the altered outer membrane protein
462 profile, reduced zinc uptake, altered cell separation and increased levels of outer membrane vesicles
463 likely through direct effect on the phospholipid content of the OM and increased
464 phosphoethanolamine levels seen for the YraP mutant strain relative to the wild type strain. YraP is
465 also important for meningococcal survival in the infant rat model of meningococcal infection.
466 Given the presence of two BON domains in YraP that are proposed to be involved in phospholipid
467 binding, we propose that YraP is involved in maintaining phospholipid homeostasis in the outer
468 membrane. These findings suggest that antibodies raised by GNA2091 could interfere with outer
469 membrane homeostasis during bacterial replication *in vivo,* a mechanism that could be the basis for
470 the "*in vivo*" protective activity induced by YraP in the mouse model of infection (2). Therefore,
471 these data further support the use of YraP as vaccine antigen and suggest that YraP and its
472 homologues could be an ideal target for novel antibiotics to disrupt the outer membrane of *N.*
473 *meningitidis* or closely related bacteria.
474
475
476 **Acknowledgements**
477 KLS was supported by the Australian National Health and Medical Research Council (NHMRC CJ
478 Martin Fellowship and Career Development Fellowship). AFH was supported by a Marie Curie
479 Fellowship (PIEF-GA-2012-328377). FO, LF and SB were recipients of Novartis fellowships from
480 the PhD program of the University of Siena and Bologna, respectively.
481 This study was sponsored by Novartis Vaccines, now acquired by the GSK group of companies.

FO, FF, MG, MP, ID are employees of the GSK group of companies. Bexsero is a trademark of the GSK group of companies.

Authors Contribution

K. L. Seib and I. Delany designed research; K. L. Seib, A. F. Haag, F. Oriente, L. Fantappiè, S. Borghi, E. A. Semchenko, B. L. Schulz, F. Ferlicca and A. Taddei performed research; K. L. Seib, B. L. Schulz, M. Giuliani, M. Pizza, I. Delany analyzed data; K. L. Seib, M. Pizza, I. Delany wrote the paper.

References

1. Stephens, D. S. (2007) Conquering the meningococcus. *FEMS Microbiol. Rev.* **31**, 3-14
2. Giuliani, M. M., Adu-Bobie, J., Comanducci, M., Arico, B., Savino, S., Santini, L., Brunelli, B., Bambini, S., Biolchi, A., Capecchi, B., Cartocci, E., Ciucchi, L., Di Marcello, F., Ferlicca, F., Galli, B., Luzzi, E., Masignani, V., Serruto, D., Veggi, D., Contorni, M., Morandi, M., Bartalesi, A., Cinotti, V., Mannucci, D., Titta, F., Ovidi, E., Welsch, J. A., Granoff, D., Rappuoli, R., and Pizza, M. (2006) A universal vaccine for serogroup B meningococcus. *Proc. Natl. Acad. Sci. U. S. A.* **103**, 10834-10839
3. O'Ryan, M., Stoddard, J., Toneatto, D., Wassil, J., and Dull, P. M. (2014) A multi-component meningococcal serogroup B vaccine (4CMenB): the clinical development program. *Drugs* **74**, 15-30
4. Toneatto, D., Pizza, M., Masignani, V., and Rappuoli, R. (2017) Emerging experience with meningococcal serogroup B protein vaccines. *Expert review of vaccines* **16**, 433-451
5. Pizza, M., Scarlato, V., Masignani, V., Giuliani, M. M., Arico, B., Comanducci, M., Jennings, G. T., Baldi, L., Bartolini, E., Capecchi, B., Galeotti, C. L., Luzzi, E., Manetti, R., Marchetti, E., Mora, M., Nuti, S., Ratti, G., Santini, L., Savino, S., Scarselli, M., Storni, E., Zuo, P., Broeker, M., Hundt, E., Knapp, B., Blair, E., Mason, T., Tettelin, H., Hood, D. W., Jeffries, A. C., Saunders, N. J., Granoff, D. M., Venter, J. C., Moxon, E. R., Grandi, G., and Rappuoli, R. (2000) Identification of vaccine candidates against serogroup B meningococcus by whole-genome sequencing. *Science* **287**, 1816-1820
6. Serruto, D., Spadafina, T., Ciucchi, L., Lewis, L. A., Ram, S., Tontini, M., Santini, L., Biolchi, A., Seib, K. L., Giuliani, M. M., Donnelly, J. J., Berti, F., Savino, S., Scarselli, M., Costantino, P., Kroll, J. S., O'Dwyer, C., Qiu, J., Plaut, A. G., Moxon, R., Rappuoli, R., Pizza, M., and Arico, B. (2010) *Neisseria meningitidis* GNA2132, a heparin-binding protein that induces protective immunity in humans. *Proc. Natl. Acad. Sci. U. S. A.* **107**, 3770-3775
7. Arenas, J., Nijland, R., Rodriguez, F. J., Bosma, T. N. P., and Tommassen, J. (2012) Involvement of three meningococcal surface-exposed proteins, the heparin-binding protein NhbA, the α-peptide of IgA protease, and the autotransporter protease NalP, in initiation of biofilm formation. *Mol. Microbiol.*, n/a-n/a
8. Fagnocchi, L., Biolchi, A., Ferlicca, F., Boccadifuoco, G., Brunelli, B., Brier, S., Norais, N., Chiarot, E., Bensi, G., Kroll, J. S., Pizza, M., Donnelly, J., Giuliani, M. M., and Delany, I.

(2013) Transcriptional regulation of the nadA gene in Neisseria meningitidis impacts the prediction of coverage of a multicomponent meningococcal serogroup B vaccine. *Infect Immun* **81**, 560-569

9. Metruccio, M. M. E., Pigozzi, E., Roncarati, D., Scorza, F. B., Norais, N., Hill, S. A., Scarlato, V., and Delany, I. (2009) A Novel Phase Variation Mechanism in the Meningococcus Driven by a Ligand-Responsive Repressor and Differential Spacing of Distal Promoter Elements. *PLoS Pathogens* **5**
10. Seib, K. L., Scarselli, M., Comanducci, M., Toneatto, D., and Masignani, V. (2015) Neisseria meningitidis factor H-binding protein fHbp: a key virulence factor and vaccine antigen. *Expert review of vaccines* **14**, 841-859
11. Vacca, I., Del Tordello, E., Gasperini, G., Pezzicoli, A., Di Fede, M., Rossi Paccani, S., Marchi, S., Mubaiwa, T. D., Hartley-Tassell, L. E., Jennings, M. P., Seib, K. L., Masignani, V., Pizza, M., Serruto, D., Arico, B., and Delany, I. (2016) Neisserial Heparin Binding Antigen (NHBA) Contributes to the Adhesion of Neisseria meningitidis to Human Epithelial Cells. *PLoS One* **11**, e0162878
12. Donnarumma, D., Golfieri, G., Brier, S., Castagnini, M., Veggi, D., Bottomley, M. J., Delany, I., and Norais, N. (2015) Neisseria meningitis GNA1030 is a ubiquinone-8 binding protein. *FASEB J* **29**, 2260-2267
13. Bos, M. P., Grijpstra, J., Tommassen-van Boxtel, R., and Tommassen, J. (2014) Involvement of *Neisseria meningitidis* Lipoprotein GNA2091 in the Assembly of a Subset of Outer Membrane Proteins. *J. Biol. Chem.*
14. Seib, K. L., Oriente, F., Adu-Bobie, J., Montanari, P., Ferlicca, F., Giuliani, M. M., Rappuoli, R., Pizza, M., and Delany, I. (2010) Influence of serogroup B meningococcal vaccine antigens on growth and survival of the meningococcus in vitro and in ex vivo and in vivo models of infection. *Vaccine* **28**, 2416-2427
15. Seib, K. L., Brunelli, B., Brogioni, B., Palumbo, E., Bambini, S., Muzzi, A., DiMarcello, F., Marchi, S., van der Ende, A., Arico, B., Savino, S., Scarselli, M., Comanducci, M., Rappuoli, R., Giuliani, M. M., and Pizza, M. (2011) Characterization of diverse subvariants of the meningococcal factor H (fH) binding protein for their ability to bind fH, to mediate serum resistance, and to induce bactericidal antibodies. *Infect. Immun.* **79**, 970-981
16. Fantappie, L., Scarlato, V., and Delany, I. (2011) Identification of the in vitro target of an iron-responsive AraC-like protein from Neisseria meningitidis that is in a regulatory cascade with Fur. *Microbiology* **157**, 2235-2247
17. Wai, S. N., Takade, A., and Amako, K. (1995) The release of outer membrane vesicles from the strains of enterotoxigenic Escherichia coli. *Microbiol Immunol* **39**, 451-456
18. Bligh, E. G., and Dyer, W. J. (1959) A rapid method of total lipid extraction and purification. *Can J Biochem Physiol* **37**, 911-917
19. White, T., Bursten, S., Federighi, D., Lewis, R. A., and Nudelman, E. (1998) High-resolution separation and quantification of neutral lipid and phospholipid species in mammalian cells and sera by multi-one-dimensional thin-layer chromatography. *Anal Biochem* **258**, 109-117
20. Rahman, M. M., Kolli, V. S., Kahler, C. M., Shih, G., Stephens, D. S., and Carlson, R. W. (2000) The membrane phospholipids of Neisseria meningitidis and Neisseria gonorrhoeae as characterized by fast atom bombardment mass spectrometry. *Microbiology* **146 (Pt 8)**, 1901-1911
21. Yeats, C., and Bateman, A. (2003) The BON domain: a putative membrane-binding domain. *Trends Biochem. Sci.* **28**, 352-355
22. Tettelin, H., Saunders, N. J., Heidelberg, J., Jeffries, A. C., Nelson, K. E., Eisen, J. A., Ketchum, K. A., Hood, D. W., Peden, J. F., Dodson, R. J., Nelson, W. C., Gwinn, M. L., DeBoy, R., Peterson, J. D., Hickey, E. K., Haft, D. H., Salzberg, S. L., White, O., Fleischmann, R. D., Dougherty, B. A., Mason, T., Ciecko, A., Parksey, D. S., Blair, E., Cittone, H., Clark, E. B., Cotton, M. D., Utterback, T. R., Khouri, H., Qin, H., Vamathevan,

J., Gill, J., Scarlato, V., Masignani, V., Pizza, M., Grandi, G., Sun, L., Smith, H. O., Fraser, C. M., Moxon, E. R., Rappuoli, R., and Venter, J. C. (2000) Complete genome sequence of Neisseria meningitidis serogroup B strain MC58. *Science* **287**, 1809-1815

23. Brooke, J. S., and Valvano, M. A. (1996) Molecular cloning of the Haemophilus influenzae gmhA (lpcA) gene encoding a phosphoheptose isomerase required for lipooligosaccharide biosynthesis. *J Bacteriol* **178**, 3339-3341
24. Pawlik, M. C., Hubert, K., Joseph, B., Claus, H., Schoen, C., and Vogel, U. (2012) The Zinc-Responsive Regulon of Neisseria meningitidis Comprises 17 Genes under Control of a Zur Element. *J Bacteriol* **194**, 6594-6603
25. Wu, H. J., Seib, K. L., Srikhanta, Y. N., Kidd, S. P., Edwards, J. L., Maguire, T. L., Grimmond, S. M., Apicella, M. A., McEwan, A. G., and Jennings, M. P. (2006) PerR controls Mn-dependent resistance to oxidative stress in Neisseria gonorrhoeae. *Mol Microbiol* **60**, 401-416
26. Delany, I., Grifantini, R., Bartolini, E., Rappuoli, R., and Scarlato, V. (2006) Effect of Neisseria meningitidis fur mutations on global control of gene transcription. *J Bacteriol* **188**, 2483-2492
27. Delany, I., Rappuoli, R., and Scarlato, V. (2004) Fur functions as an activator and as a repressor of putative virulence genes in Neisseria meningitidis. *Mol Microbiol* **52**, 1081-1090
28. Stork, M., Bos, M. P., Jongerius, I., de Kok, N., Schilders, I., Weynants, V. E., Poolman, J. T., and Tommassen, J. (2010) An outer membrane receptor of Neisseria meningitidis involved in zinc acquisition with vaccine potential. *PLoS Pathog* **6**, e1000969
29. Konovalova, A., Kahne, D. E., and Silhavy, T. J. (2017) Outer Membrane Biogenesis. *Annu Rev Microbiol* **71**, 539-556
30. Bos, M. P., Robert, V., and Tommassen, J. (2007) Biogenesis of the gram-negative bacterial outer membrane. *Annu Rev Microbiol* **61**, 191-214
31. Hooda, Y., Shin, H. E., Bateman, T. J., and Moraes, T. F. (2017) Neisserial surface lipoproteins: structure, function and biogenesis. *Pathogens and Disease* **75**
32. Malinverni, J. C., and Silhavy, T. J. (2009) An ABC transport system that maintains lipid asymmetry in the gram-negative outer membrane. *Proc Natl Acad Sci U S A* **106**, 8009-8014
33. Ekiert, D. C., Bhabha, G., Isom, G. L., Greenan, G., Ovchinnikov, S., Henderson, I. R., Cox, J. S., and Vale, R. D. (2017) Architectures of Lipid Transport Systems for the Bacterial Outer Membrane. *Cell* **169**, 273-285 e217
34. Muzzi, A., Mora, M., Pizza, M., Rappuoli, R., and Donati, C. (2013) Conservation of meningococcal antigens in the genus Neisseria. *MBio* **4**, e00163-00113
35. Jacobsson, S., Hedberg, S. T., Molling, P., Unemo, M., Comanducci, M., Rappuoli, R., and Olcen, P. (2009) Prevalence and sequence variations of the genes encoding the five antigens included in the novel 5CVMB vaccine covering group B meningococcal disease. *Vaccine* **27**, 1579-1584
36. Hadad, R., Jacobsson, S., Pizza, M., Rappuoli, R., Fredlund, H., Olcen, P., and Unemo, M. (2012) Novel meningococcal 4CMenB vaccine antigens - prevalence and polymorphisms of the encoding genes in Neisseria gonorrhoeae. *APMIS* **120**, 750-760
37. Lappann, M., Otto, A., Brauer, M., Becher, D., Vogel, U., and Johswich, K. (2016) Impact of Moderate Temperature Changes on Neisseria meningitidis Adhesion Phenotypes and Proteome. *Infection and immunity* **84**, 3484-3495
38. Echenique-Rivera, H., Muzzi, A., Del Tordello, E., Seib, K. L., Francois, P., Rappuoli, R., Pizza, M., and Serruto, D. (2011) Transcriptome Analysis of *Neisseria meningitidis* in Human Whole Blood and Mutagenesis Studies Identify Virulence Factors Involved in Blood Survival. *PLoS Pathogens* **7**
39. Yim, H. H., and Villarejo, M. (1992) osmY, a new hyperosmotically inducible gene, encodes a periplasmic protein in Escherichia coli. *Journal of bacteriology* **174**, 3637-3644

40. Onufryk, C., Crouch, M. L., Fang, F. C., and Gross, C. A. (2005) Characterization of six lipoproteins in the sigmaE regulon. *J. Bacteriol.* **187**, 4552-4561
41. Volokhina, E. B., Grijpstra, J., Stork, M., Schilders, I., Tommassen, J., and Bos, M. P. (2011) Role of the periplasmic chaperones Skp, SurA, and DegQ in outer membrane protein biogenesis in *Neisseria meningitidis*. *J. Bacteriol.* **193**, 1612-1621
42. Tsang, M. J., Yakhnina, A. A., and Bernhardt, T. G. (2017) NlpD links cell wall remodeling and outer membrane invagination during cytokinesis in Escherichia coli. *PLoS genetics* **13**, e1006888
43. Lenz, J. D., Stohl, E. A., Robertson, R. M., Hackett, K. T., Fisher, K., Xiong, K., Lee, M., Hesek, D., Mobashery, S., Seifert, H. S., Davies, C., and Dillard, J. P. (2016) Amidase Activity of AmiC Controls Cell Separation and Stem Peptide Release and Is Enhanced by NlpD in Neisseria gonorrhoeae. *J Biol Chem* **291**, 10916-10933
44. Ercoli, G., Tani, C., Pezzicoli, A., Vacca, I., Martinelli, M., Pecetta, S., Petracca, R., Rappuoli, R., Pizza, M., Norais, N., Soriani, M., and Arico, B. (2015) LytM proteins play a crucial role in cell separation, outer membrane composition, and pathogenesis in nontypeable Haemophilus influenzae. *MBio* **6**, e02575
45. Adu-Bobie, J., Lupetti, P., Brunelli, B., Granoff, D., Norais, N., Ferrari, G., Grandi, G., Rappuoli, R., and Pizza, M. (2004) GNA33 of Neisseria meningitidis is a lipoprotein required for cell separation, membrane architecture, and virulence. *Infect Immun* **72**, 1914-1919
46. Dowhan, W. (2013) A retrospective: use of Escherichia coli as a vehicle to study phospholipid synthesis and function. *Biochim Biophys Acta* **1831**, 471-494
47. Roier, S., Zingl, F. G., Cakar, F., Durakovic, S., Kohl, P., Eichmann, T. O., Klug, L., Gadermaier, B., Weinzerl, K., Prassl, R., Lass, A., Daum, G., Reidl, J., Feldman, M. F., and Schild, S. (2016) A novel mechanism for the biogenesis of outer membrane vesicles in Gram-negative bacteria. *Nat Commun* **7**, 10515
48. Morris, F. C., Wells, T. J., Bryant, J. A., Schager, A. E., Sevastsyanovich, Y. R., Squire, D. J. P., Marshall, J., Isom, G. L., Rooke, J., Maderbocus, R., Knowles, T. J., Overduin, M., Rossiter, A. E., Cunningham, A. F., and Henderson, I. R. (2018) YraP Contributes to Cell Envelope Integrity and Virulence of Salmonella enterica Serovar Typhimurium. *Infect Immun* **86**
49. Yeats, C., and Bateman, A. (2003) The BON domain: a putative membrane-binding domain. *Trends Biochem Sci* **28**, 352-355
50. Bogdanov, M., Umeda, M., and Dowhan, W. (1999) Phospholipid-assisted refolding of an integral membrane protein. Minimum structural features for phosphatidylethanolamine to act as a molecular chaperone. *The Journal of biological chemistry* **274**, 12339-12345
51. Patel, G. J., and Kleinschmidt, J. H. (2013) The lipid bilayer-inserted membrane protein BamA of Escherichia coli facilitates insertion and folding of outer membrane protein A from its complex with Skp. *Biochemistry* **52**, 3974-3986
52. Vitrac, H., MacLean, D. M., Jayaraman, V., Bogdanov, M., and Dowhan, W. (2015) Dynamic membrane protein topological switching upon changes in phospholipid environment. *Proc Natl Acad Sci U S A* **112**, 13874-13879
53. Bogdanov, M., and Dowhan, W. (1998) Phospholipid-assisted protein folding: phosphatidylethanolamine is required at a late step of the conformational maturation of the polytopic membrane protein lactose permease. *EMBO J* **17**, 5255-5264
54. Bogdanov, M., and Dowhan, W. (1995) Phosphatidylethanolamine is required for in vivo function of the membrane-associated lactose permease of Escherichia coli. *The Journal of biological chemistry* **270**, 732-739
55. Binder, H., Arnold, K., Ulrich, A. S., and Zschornig, O. (2001) Interaction of Zn2+ with phospholipid membranes. *Biophys Chem* **90**, 57-74
56. Barfield, K. D., and Bevan, D. R. (1985) Fusion of phospholipid vesicles induced by Zn2+, Cd2+, and Hg2+. *Biochemical and biophysical research communications* **128**, 389-395

679 57. Carman, G. M., and Han, G. S. (2007) Regulation of phospholipid synthesis in
680 Saccharomyces cerevisiae by zinc depletion. *Biochim Biophys Acta* **1771**, 322-330
681

Figure Legends

Figure 1: Characterisation of the GNA2091 locus. (A) Representation of the GNA2091 protein. The leader peptide and predicted LipoP signal are shown, as well as the BON and OsmY protein domain predictions from Pfam and NCBI Conserved Domain database. **(B)** Representation of the genome locus of NMB2091 in *N. meningitidis* strain MC58. The open reading frames are shown by arrows, with the NMB locus number inside the arrow, and the annotated gene function above the arrow. **(C)** Investigation of the *nmb2089-2092* operon. Reverse transcriptase (RT)-PCR of the *NMB2089-NMB2092* region in meningococcal strain MC58, demonstrated that *nmb2091* is co-transcribed with adjacent genes. The locations of PCR primers are shown, as well as the PCR products from cDNA, and the negative (no reverse transcriptase (no RT) and water (H_2O)) and positive (genomic DNA (gDNA)) controls. **(D)** Representative organization of homologues of NMB2089-2091 from various Gram-negative organisms. Protein sequences were aligned in ClustalW and visualized with JalView [identical nucleotides are shown as vertical lines, with identity over a run of nucleotides shown as dark gray (>80% identity), light gray (<50%), or white (<50% identity or a gap)]. The genome loci of aligned proteins is indicated on the left, and is from NMB, *Neisseria meningitidis* MC58; ECP, *Escherichia coli* 536; STY, *Salmonella enterica* subsp. enterica serovar Typhi str. CT18; VC, *Vibrio cholerae* O1 biovar El Tor str. N16961; PM, *Pasteurella multocida* subsp. multocida str. Pm70; LP, *Legionella pneumophila* subsp. pneumophila str. Philadelphia 1; HI, *Haemophilus influenzae* Rd KW20.

Figure 2. The Δ2091 mutant strain displays increased bacterial aggregation. Bacterial growth in GC broth (A) and formation of bacterial aggregates were analyzed by **(B)** colony counts and **(C)** scanning electron microscopy. **(A)** Growth rates of MC58 wild type, the Δ2091mutant and C-2091 complemented strains were assessed by optical density (OD) at 600 nm. **(B)** Single colonies of the wild type, mutant and complemented strains were selected, serially diluted and plated to determine CFU per colony. Student's t-test p-value; 0.00003 for wild type vs. mutant, 0.191 for wild type vs. complemented strain. Experiments were performed with six colonies on at least three occasions and representative results are shown. **(C)** Scanning electron micrographs of the wild type, mutant and complemented strains, showing mainly diplococci for the wild type and complement strains, while several aggregates are seen for the Δ2091 mutant strain. **(D)** Thin section transmission electron micrographs of the wild type, mutant and complemented strains, showing mainly individual or diplococci for the wild type and complement strains while the GNA2091 mutant shows a mild cell separation phenotype and can manifest as triple and quadruple cells per group. Images are representative of multiple fields at x 5,600 magnification, whereas the different coccoid multimers that can be present in each strain are highlighted at x 15,000 magnification.

Figure 3. The Δ2091 mutant strain has altered outer membrane protein and outer membrane vesicle (OMV) formation. Coomassie stained SDS-PAGE and Western blot analysis with polyclonal mouse sera raised to OMVs of **(A)** whole-cell lysates and **(B)** OMVs of MC58 wild type, the Δ2091mutant and C-2091 complemented strains. **(C)** The OMV yields of overnight cultures of the wild type, mutant and complemented strains, based on total protein concentration in OMV preparations. **(D)** Scanning electron micrographs of the wild type, mutant and complemented strains, showing hypervesiculation of the Δ2091 mutant strain.

Figure 4. The Δ2091 mutant strain has altered phospholipid formation as shown by thin layer chromatography (TLC) and mass spectrometry (MS). (A) TLC analysis of phospholipid extracts from OMV preparations of the defined strains. PG, phosphatidylglycerol; PE, phosphatidylethanolamine; PA, phosphatidic acid. **(B)** Negative ion mode MS/MS all total ion trace for lipids extracted from wild type (black), Δ2091mutant (red), and C-2091 complemented (black dash) strains. Inset shows *m/z* region around the 688.5 Da peak. **(C)** MS/MS of species at an *m/z* of 688.5 Da. **(D)** Cartoon structure of PE(16:1(9Z)/16:0), consistent with MS/MS in **(C).**

Figure 5: GNA2091 is involved in zinc homeostasis. (A) Growth rates of MC58 wild type, the Δ2091mutant and C-2091 complemented strains in Mueller Hinton (MH) broth (left) and MH supplemented with zinc (right). Growth rates were assessed by optical density (OD) at 600 nm over 7 hours. **(B)** Summary of DNA microarray results, showing altered gene expression between the Δ2091 and wild type strains and the overlap of regulated genes that are present in the *Neisseria* Zur and Fur regulons, and other genes involved in metabolism. The list of genes with ≥2 fold altered expression between the MC58 wild type, the Δ2091mutant strains is shown in Table S2. **(C)** Quantitative real-time (qRT)-PCR of *znuD* expression MC58 wild type, Δ2091mutant and C-2091 complemented strains in MH broth +/- zinc.

Figure 6. GNA2091 is required for optimal survival in an infant rat model of infection.
Infant rats were infected intraperitoneally with an infectious dose of **(A)** $1x10^3$, $1x10^4$, or $1x10^5$ colony forming units (CFU) of *N. meningitidis* 2996 wild type and Δ2091 mutant strains, or **(B)** $1x10^4$ CFU C-2091 complemented and Δ2091 mutant strains, at a 1:1 ratio. At 18 h post-injection blood was collected and serial dilutions were plated and bacterial colonies were counted. The competitive index (CI) for individual rats are shown as well as the mean and median for each infectious dose. The CI was calculated as follows, CI = (wild type CFU recovered / mutant CFU recovered) / (wild type inoculum /mutant inoculum). The p-values using the Wilcoxon Signed-Ranks Test for the survival of the mutant strain with respect to the isogenic wild type parent strain are 0.0047, <0.0001 and 0.0001 for the dose of $1x10^3$, $1x10^4$, and $1x10^5$, respectively. The p-value for the mutant strain with respect to the complemented strain is 0.0434.

Table S1 Oligonucleotides used in this study.

Name	Sequence
2089rtF	CGGCATGATTCTGTTTGTTG
2090rtF	ACGACTACGGTTTCGACCAC
2090rtR	GTGGAAATGCCGACCAATAC
2091rtF2	ACGTTATGGCGTTGCGTAT
2091rtR2	TGTAGCCTTTGGTTTGGTTG
2092rtF	TGACCCCCAAACTCCTGATA
2092rtR	GGTTGAATGTGCTGACGATG
2093rtF	ATGAACGGCATCATCATCAA
2093rtR	CGAATTGTCCGATGTAGTCG
2093rtF	CACTGGGCGACGTAGGTTAC
1475rtF	ACGGCAGTTACCTCGTCATC
1475rtR	ATAGCTTGCGTCAGGCATTT
0941rtF	TCAAAACCGCCAAACAACG
0941rtR	GCGCTTTAAAACGCGGATTG
znuDrtF	GCATCCACGCTTCGCAATA
znuDrtR	TTTCGCCGTGATGGTTCAA
0634rtF	TCTATCCGATACGCACTGCT
0634rtR	TGTGCTGCTTCTTTGTGTTG
16SRT_F	ACGGAGGGTGCGAGCGTTAATC
16SRT_R	CTGCCTTCGCCTTCGGTATTCCT

Table S2. Differentially expressed genes from microarray studies of MC58 wild type and Δ2091 mutant strains.

Regulated Genes		DNA Microarray Fold change [a]		qRT-PCR Fold change [b]	
MC58 Gene	**Gene Function, Name**	**Δ2091 vs. WT**	**P-val**	**Δ2091 vs WT**	**Δ2091 vs C2091**
Up regulated in Δ2091					
NMB1475[c]	conserved hypothetical protein, *hyp.*	8.8	2.1E-06	4.4 *	0.5
NMB0942[c]	50S ribosomal protein L31, *rpmE2*	5.7	1.5E-05		
NMB0941[c]	50S ribosomal protein L36, *rpmJ2*	5.5	7.2E-04	8.0	1.0
NMB0964[c]	TonB-dependent Zn receptor, *znuD*	5.4	1.6E-03	6.8 *	1.0
NMB2092[e]	hypothetical protein	3.6	4.9E-07	*3.2*	*4.9*
NMB2093[e]	methionine aminopeptidase, *map*	2.8	1.8E-05	*2.0*	*3.0*
NMB2039	porin, *porB*	2.5	1.3E-03		
NMB1988[d]	Fe transporter, *fetA /frpB*	2.4	3.8E-04	*	
NMB0028	hypothetical protein	2.4	9.3E-03		
NMB0744[d]	hypothetical protein	2.3	8.5E-05		
NMB0634[d]	Fe ABC transporter, *fbpA*	2.2	1.8E-04	1.7	1.0
NMB1377[d]	L-lactate dehydrogenase, *lldA*	2.1	1.6E-04		
NMB1458[d]	fumarate hydratase, class II, aerobic, *fumC*	2.1	0.0E+00		
NMB0317[c]	conserved hypothetical protein	2.1	2.3E-02		
NMB0586[c]	Mn/Zn ABC transporter, periplasmic binding protein, *mntC*	1.9	1.2E-03	*	
Down regulated in Δ2091					
NMB0378	putative phosphate permease	2.0	5.8E-03		
NMB1938	ATP synthase F0, *atpF*	2.1	3.1E-03		
NMB0431	methylcitrate synthase, *prpC*	2.5	2.6E-03		
NMB0430	putative carboxyphosphonoenol-pyruvate phosphonomutase, *prpB*	2.6	1.4E-03		
NMB2091	GNA2091	59.2	0.0E+00	*	

[a] Average fold change from three separate microarray experiments including a dye swap experiment (cut off, an average of ≥2 fold change and p-value ≤ 0.05).

[b] Average fold change from three separate experiments. * Differential expression confirmed by Western blot or flow cytometry analysis (data not shown).

[c] Members of the *N. meningitidis* (24) or *N. gonorrhoeae* (25) Zur regulons. NB, other genes from the *N. meningitidis* Zur regulon (24) were also altered but below the cut-off threshold used; NMB0588 (*mntA*, 1.5 fold increased expression in GNA2091, P value 0.012); NMB0587 (*mntB*, 1.4, P value 0.08) and NMB0820 (hyp, 1.5, P value 0.017); NMB0546 (*adhP*, 1.7 fold decreased expression in GNA2091; P value 0.013).

[d] Members of the Fur regulon (repressed by Fur and Fe).

[e] The altered regulation of these genes cannot be directly attributed to the role of GNA2091. NMB2092 and NMB2093 are downstream of, and co-transcribed with NMB2091, and their expression is not restored to wild type level in the C-2091 complemented strain.

Figure 1

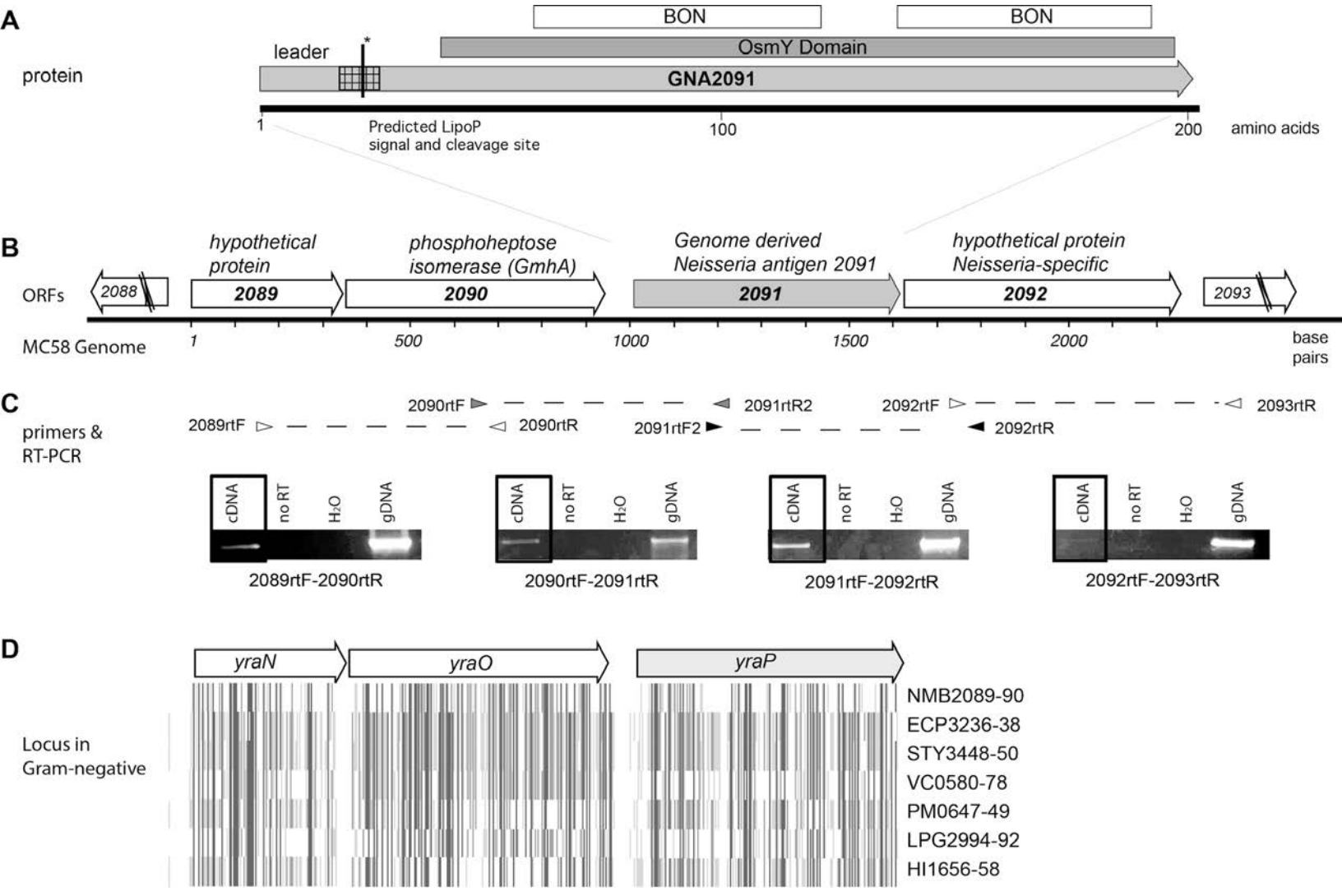
A
protein
BON
BON
OsmY Domain
leader
GNA2091
1
Predicted LipoP
signal and cleavage site
100
200
amino acids
B
ORFs
MC58 Genome
2088
hypothetical protein
2089
phosphoheptose isomerase (GmhA)
2090
Genome derived Neisseria antigen 2091
2091
hypothetical protein Neisseria-specific
2092
2093
1
500
1000
1500
2000
base pairs
C
primers & RT-PCR
2089rtF
2090rtR
2090rtF
2091rtR2
2091rtF2
2092rtR
2092rtF
2093rtR
cDNA
no RT
H2O
gDNA
2089rtF-2090rtR
2090rtF-2091rtR
2091rtF-2092rtR
2092rtF-2093rtR
D
Locus in Gram-negative
yraN
yraO
yraP
NMB2089-90
ECP3236-38
STY3448-50
VC0580-78
PM0647-49
LPG2994-92
HI1656-58

Figure 2

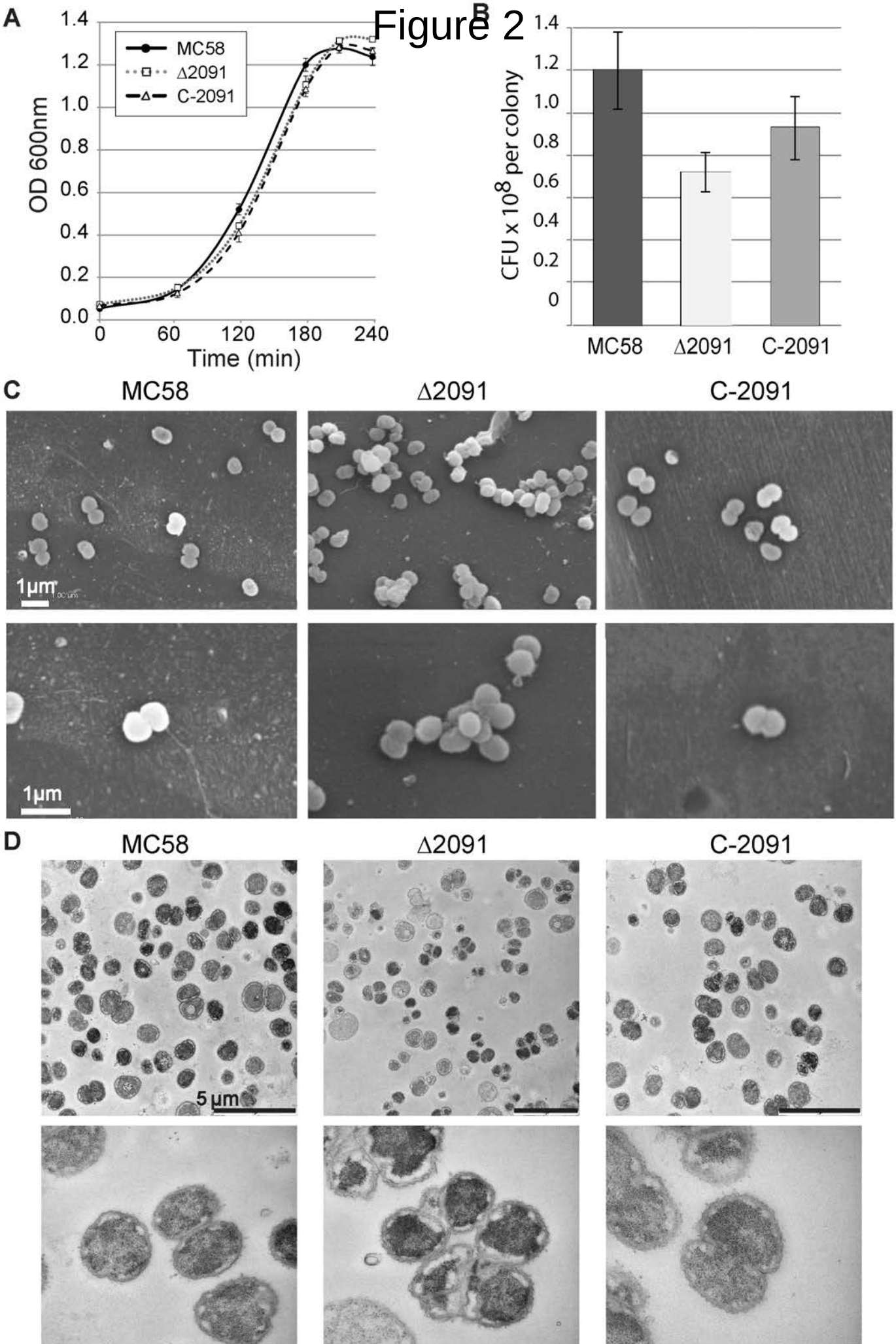
A
MC58
Δ2091
C-2091
OD 600nm
Time (min)
B
CFU x 10^8 per colony
MC58
Δ2091
C-2091
C
MC58
Δ2091
C-2091
1μm
1μm
D
MC58
Δ2091
C-2091
5 μm
1μm

Figure 3

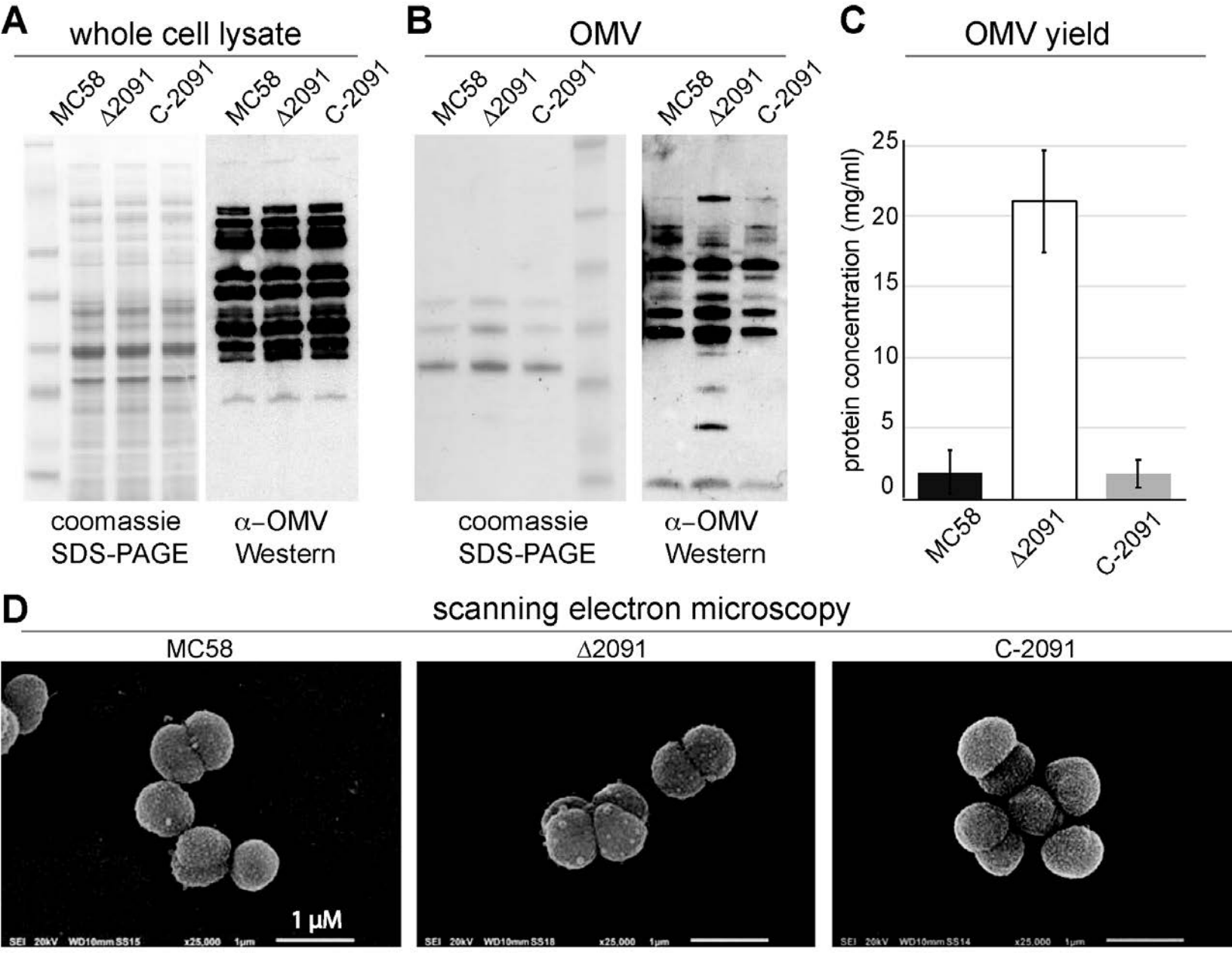
A
whole cell lysate
MC58
Δ2091
C-2091
MC58
Δ2091
C-2091
coomassie
SDS-PAGE
α–OMV
Western
B
OMV
MC58
Δ2091
C-2091
MC58
Δ2091
C-2091
coomassie
SDS-PAGE
α–OMV
Western
C
OMV yield
protein concentration (mg/ml)
25
20
15
10
5
0
MC58
Δ2091
C-2091
D
scanning electron microscopy
MC58
Δ2091
C-2091
1 µM

Figure 4

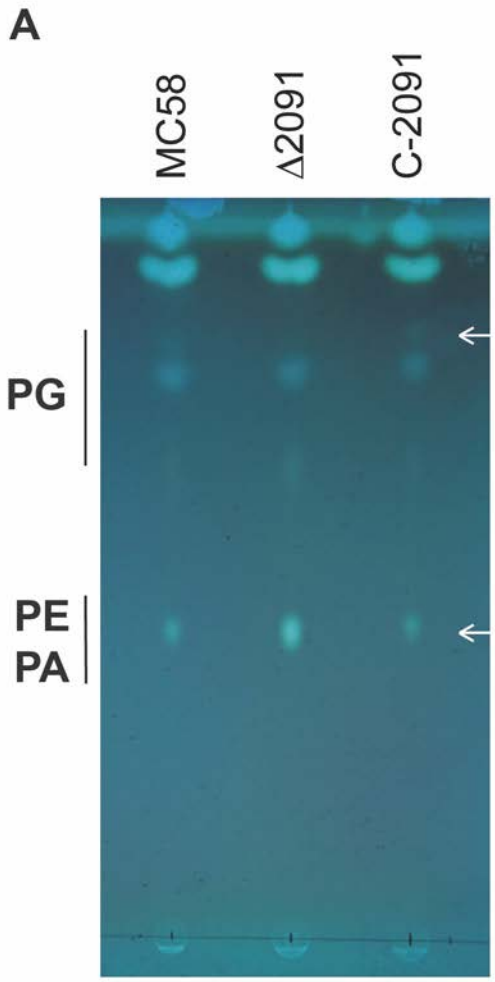
A
MC58
Δ2091
C-2091
PG
PE
PA

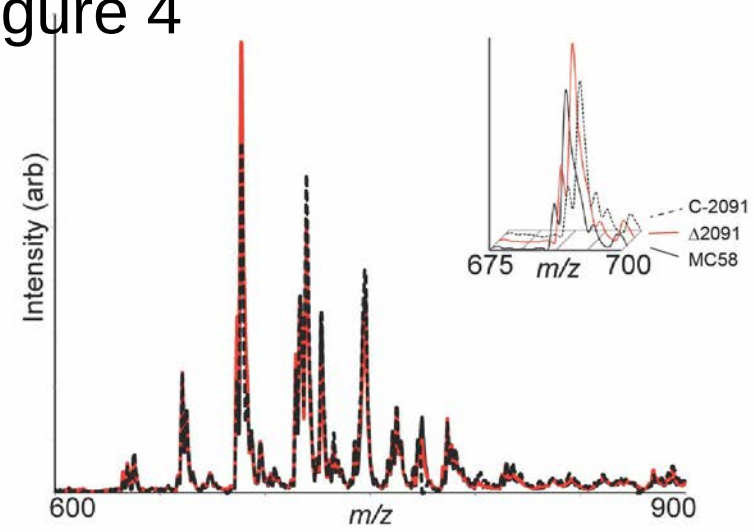
B
Intensity (arb)
600
m/z
900
675
m/z
700
C-2091
Δ2091
MC58

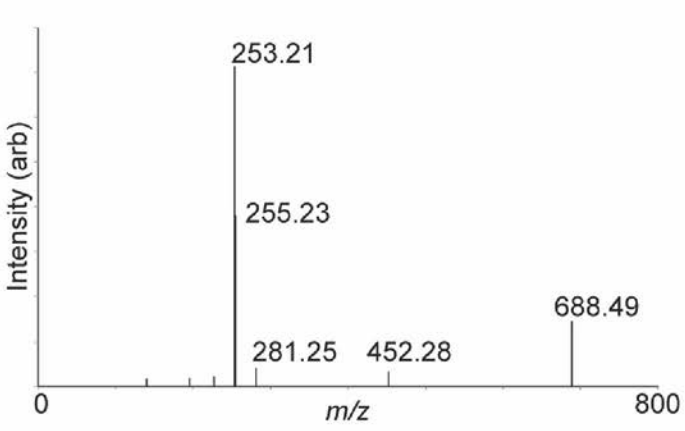
C
Intensity (arb)
253.21
255.23
688.49
281.25
452.28
0
m/z
800

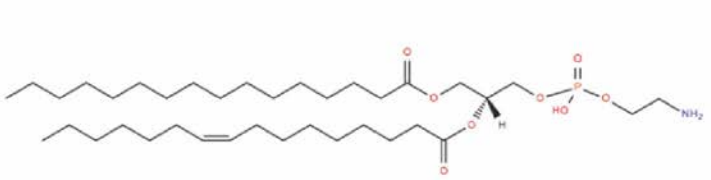
D

Figure 5

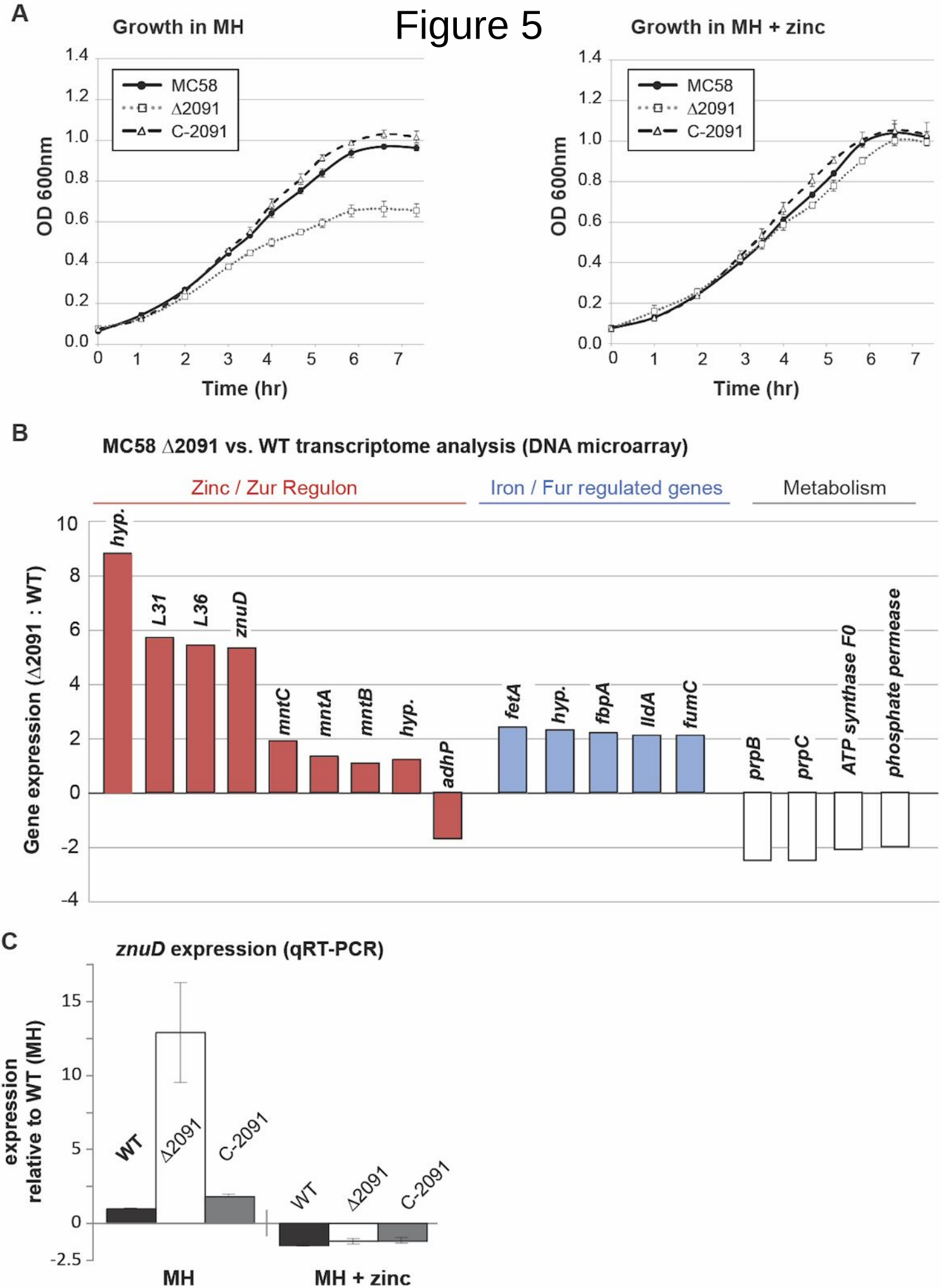
A
Growth in MH
MC58
Δ2091
C-2091
OD 600nm
Time (hr)
Growth in MH + zinc
B
MC58 Δ2091 vs. WT transcriptome analysis (DNA microarray)
Zinc / Zur Regulon
Iron / Fur regulated genes
Metabolism
Gene expression (Δ2091 : WT)
hyp.
L31
L36
znuD
mntC
mntA
mntB
hyp.
adhP
fetA
hyp.
fbpA
lldA
fumC
prpB
prpC
ATP synthase F0
phosphate permease
C
znuD expression (qRT-PCR)
expression relative to WT (MH)
WT
Δ2091
C-2091
MH
MH + zinc

Figure 6

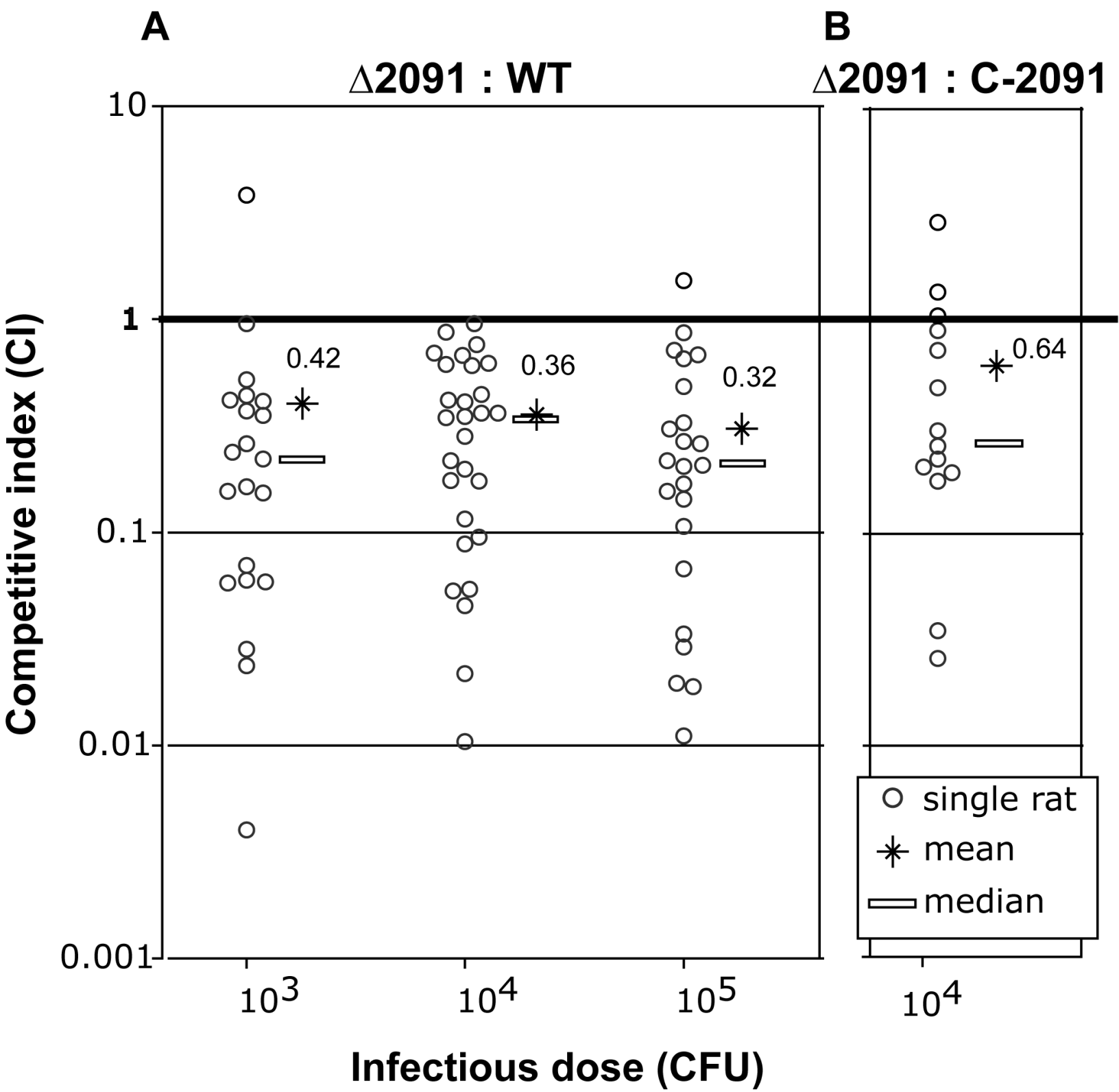
A
Δ2091 : WT
B
Δ2091 : C-2091
10
1
0.1
0.01
0.001
Competitive index (CI)
0.42
0.36
0.32
0.64
single rat
mean
median
10^3
10^4
10^5
10^4
Infectious dose (CFU)